Laser Science and Development

Generation of joule-level green bursts of nanosecond pulses from a DPSSL amplifier

A new approach to generation of a burst of high-energy green pulses by placing a high-energy multi-slab Yb:YAG DPSSL amplifier and SHG crystal inside a regenerative cavity is presented. In a proof-of-concept test, stable generation of a burst of six green (515 nm) pulses, each 10 ns in duration and separated by 29.4 ns (34 MHz), with 2.0 J total energy has been demonstrated at 1 Hz from a non-optimized ring cavity design. A maximum individual green pulse energy of 580 mJ was produced from a 1.78 J circulating infrared (1030 nm) pulse (average fluence 0.9 J/cm^2), corresponding to a SHG conversion efficiency of 32%. Experimental results have been compared with predicted performance from a simple model. Efficient generation of a burst of high energy green pulses offers an attractive pump source for Ti:Sa amplifiers, providing the potential to reduce the impact of amplified stimulated emission by reducing instantaneous transverse gain.

Authors: P.D. Mason, H. Barrett, S. Banerjee, T.J. Butcher, J.L. Collier

Contact author: P.D. Mason (paul.mason@stfc.ac.uk)

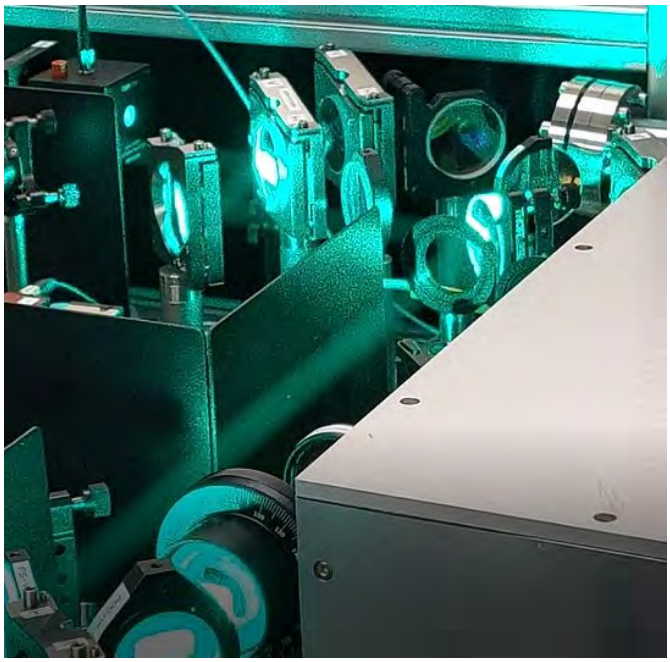

Modelling of thermally-induced stress birefringence in a 10 J, 100 Hz diode-pumped Yb:YAG laser

The high heat loads intrinsically associated with high energy, high repetition rate operation require sophisticated thermal management analyses to minimise the impact of thermal effects on laser performance. In particular, non-uniform heat deposition in optical components can lead to thermal aberrations and thermally-induced stress birefringence. This results in depolarisation of the beam, a deterioration of polarisation purity of a beam passing through the affected optic.

We present an overview and the results of thermal stress-induced depolarisation modelling of Yb:YAG gain medium slabs in a multipass, cryogenically-cooled, nanosecond, diode-pumped solid state laser operating at 10 J, 100 Hz for various input polarisation states. We expect these results to aid in the optimisation of future laser systems.

Authors: G. Quinn, D. Clarke, M. De Vido

Contact author: G. Quinn (gary.quinn@stfc.ac.uk)

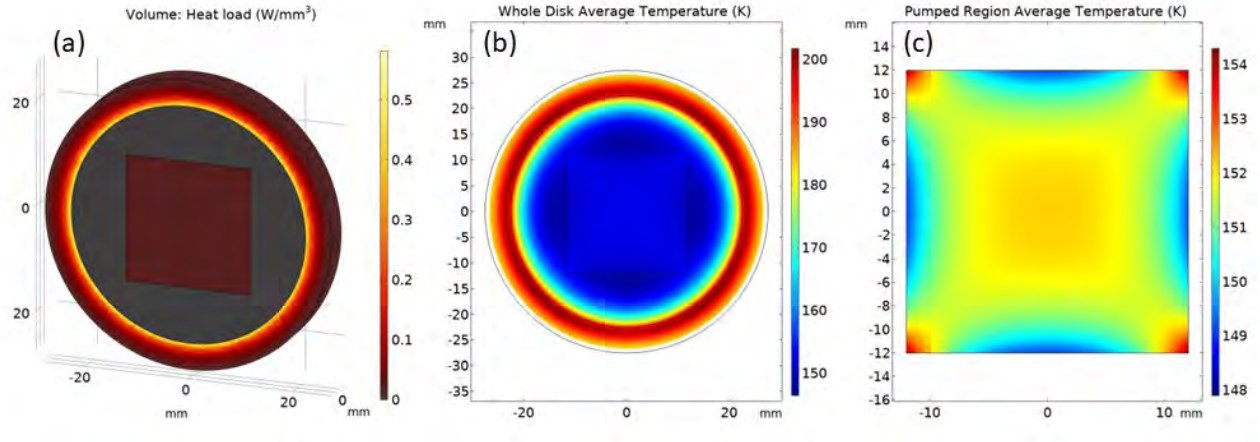

Figure 1: Simulation results showing the heat load distribution within the gain medium slab (a), the temperature distribution in the whole slab averaged over thickness (b), and the temperature distribution in the pumped region averaged over thickness (c)

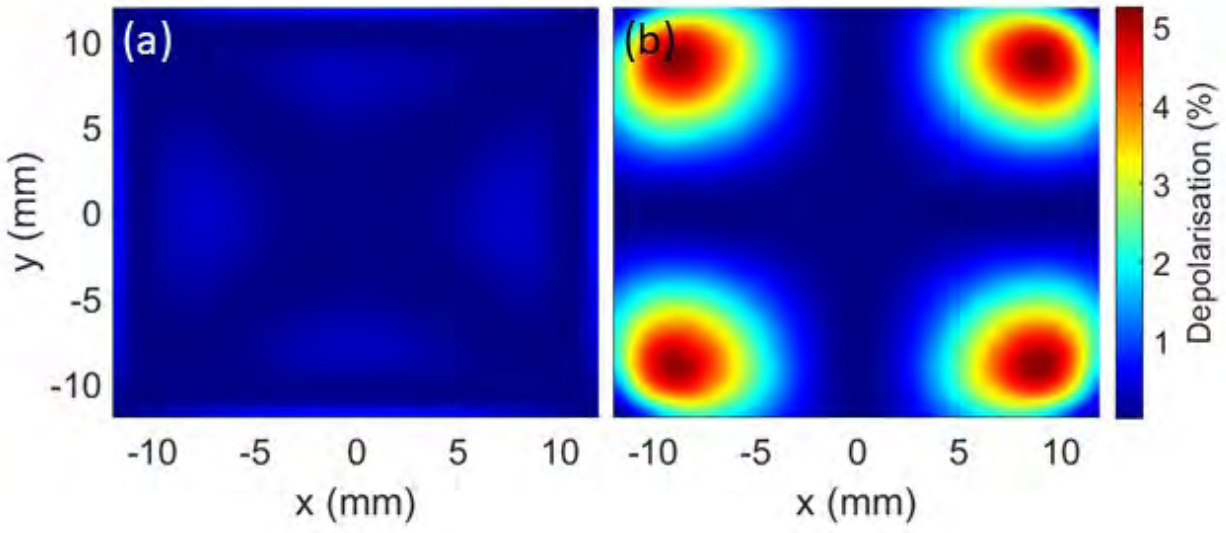

Figure 2: Simulation results showing the single pass depolarisation of a beam propagating through the six gain medium slabs in the amplifier head with an input polarisation state of 45° (a), and 0° (b)

Damage resilience testing of broadband thin-film coating for use in a high-energy Ti:Sa amplifier system

EPAC is a new research facility currently under development at the STFC Central Laser Facility in the UK. It will house a titanium-doped sapphire laser amplifier that will operate at a 10 Hz repetition rate to deliver compressed pulses of PW peak power for applications of laser-driven radiation and particle sources. To achieve this high power, it is key that optics are resilient to laser induced damage. We are performing independent in-house damage resilience tests to ensure that our standards are met.

We report results for broadband highly reflective coatings for the EPAC Ti:Sa amplifier, comparing samples from different suppliers and deposition techniques.

Authors: A.M. Wojtusiak, P.D. Mason, N. Bourgeois, R. Pattathil, C. Hernandez-Gomez

Contact author: A.M. Wojtusiak (agnieszka.wojtusiak@stfc.ac.uk)

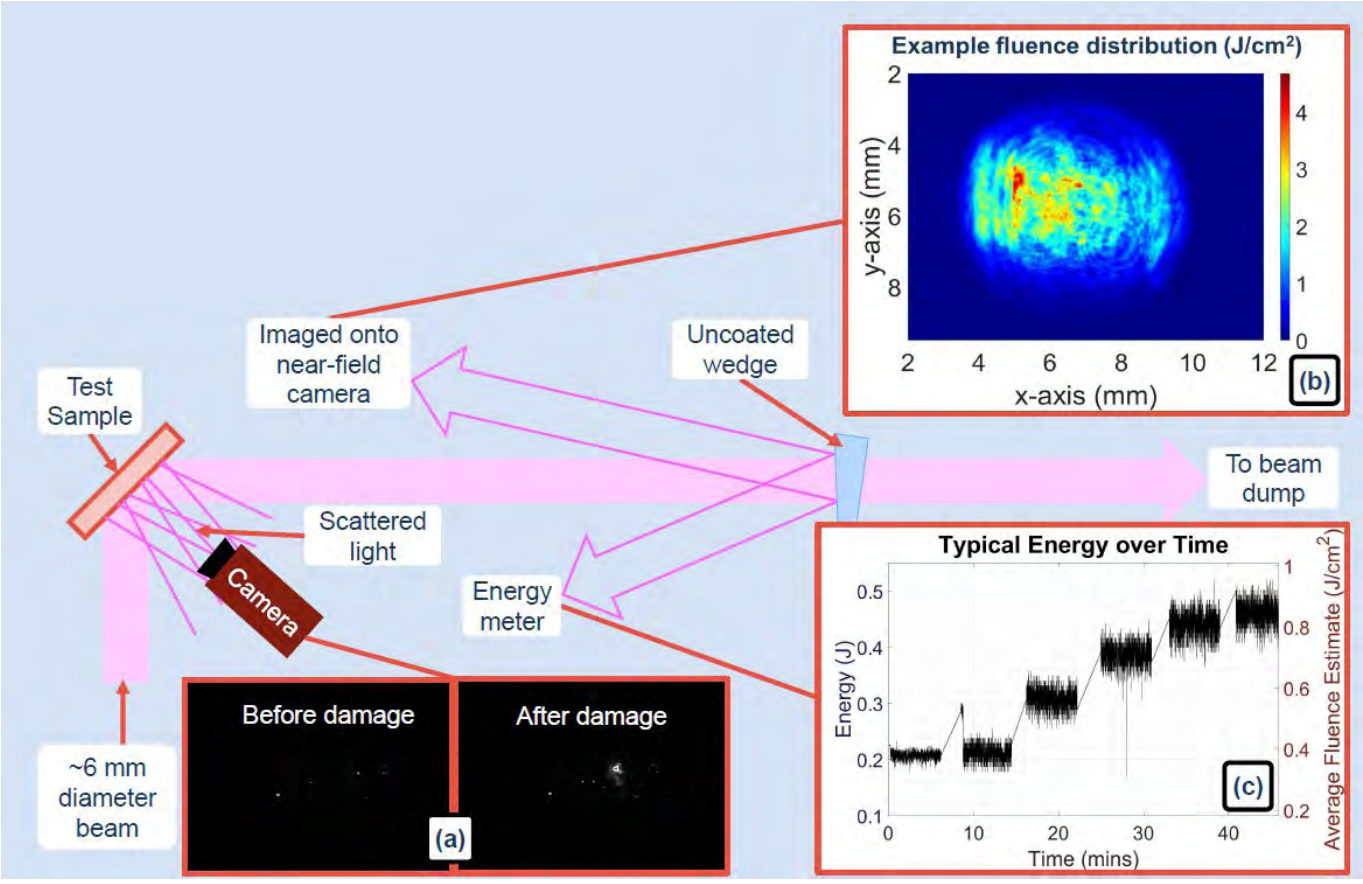

The key components of the test setup are shown here.

A CCD camera imaging light directly scattered from the test sample is used to detect initiation of damage. Insert (a) shows a typical view before and after damage has occurred.

Insert (b) shows an example of the beam profile that is relay imaged from the test sample onto another CCD camera. It also shows the fluence distribution for the maximum incident energy for that sample.

Insert (c) shows a typical graph of pulse energy over time, as well as an estimate of the average fluence – calculated by dividing the pulse energy by an estimate of the beam area.

High-integrity laser safety shutters for personnel interlocks

During the expansion of the Artemis facility, it emerged that innovative beam shutters were required to ensure safety across interconnected spaces. Specifically, wall-mounted shutters were needed to manage and block laser beam propagation between adjacent rooms, and a table/enclosure-mounted shutter variant was also needed for the optical tables. After a detailed specification process, it became apparent that there were no suitable commercial solutions, so a proprietary design was developed.

This new design features compact, lightweight, non-contact switches that are compatible with the CLF's high-integrity laser interlock safety system. These switches are used to monitor the open and closed states of a shutter's actuator. Extensive testing, encompassing nearly 600,000 simulated operations, has demonstrated that the shutters should be able to provide around 287 years of operation without the need for maintenance.

This innovative solution not only enhances operational longevity, but also aligns with the stringent safety requirements of advanced laser facilities.

Authors: S. Spurdle, R. Bickerton, T. Masarira

Contact author: R. Bickerton (richard.bickerton@stfc.ac.uk)

Figure 1: Wall-mounted shutter design

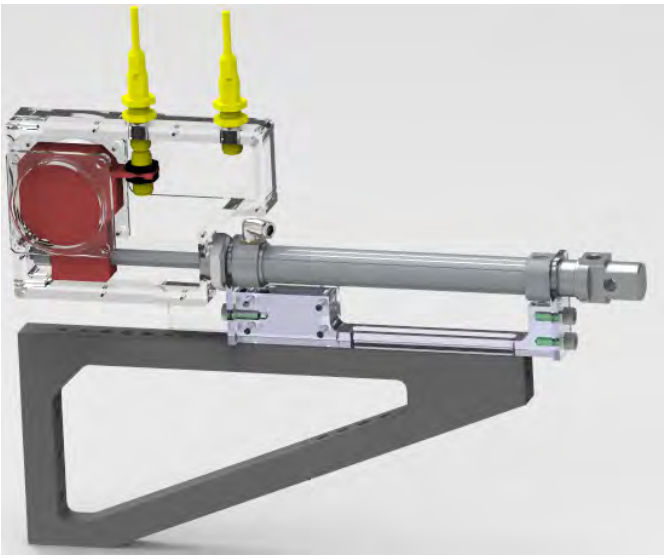

Figure 2: Table/enclosure-mounted shutter design

Laser diagnostic design for the EPAC EA1 beamline

Experimental Area 1 will house a long-focus PW laser beamline primarily designed for laser-wakefield acceleration, as reported in the previous CLF annual report.[1] Here, we describe the diagnostics that will be used to characterise and monitor the laser beam. The first measures the properties of the beam entering EA1, by taking a leakage through the final turning mirror in the beamline. The second characterises the laser pulse exiting the target, to provide spectral and spatial measurements of the beam after the plasma interaction. The optical arrangement attenuates and down-sizes the beam, then relay images onto near-field and far-field cameras, wavefront sensors, spectrometers, and energy meters.

The set-ups have been designed so that they can work both with low-power alignment modes and with the full laser energy. In this way they can be used for daily alignment as well as acting as on-shot references. Zemax software has been used to ensure aberration-free performance of the optical system.

[1] *D.R. Symes et al. EPAC Experimental Areas and Targetry Developments. CLF Ann. Rep. 2021-2022*

Authors: T. Dzelzainis, A. Stallwood, D.R. Symes

Contact author: T. Dzelzainis (thomas.dzelzainis@stfc.ac.uk)

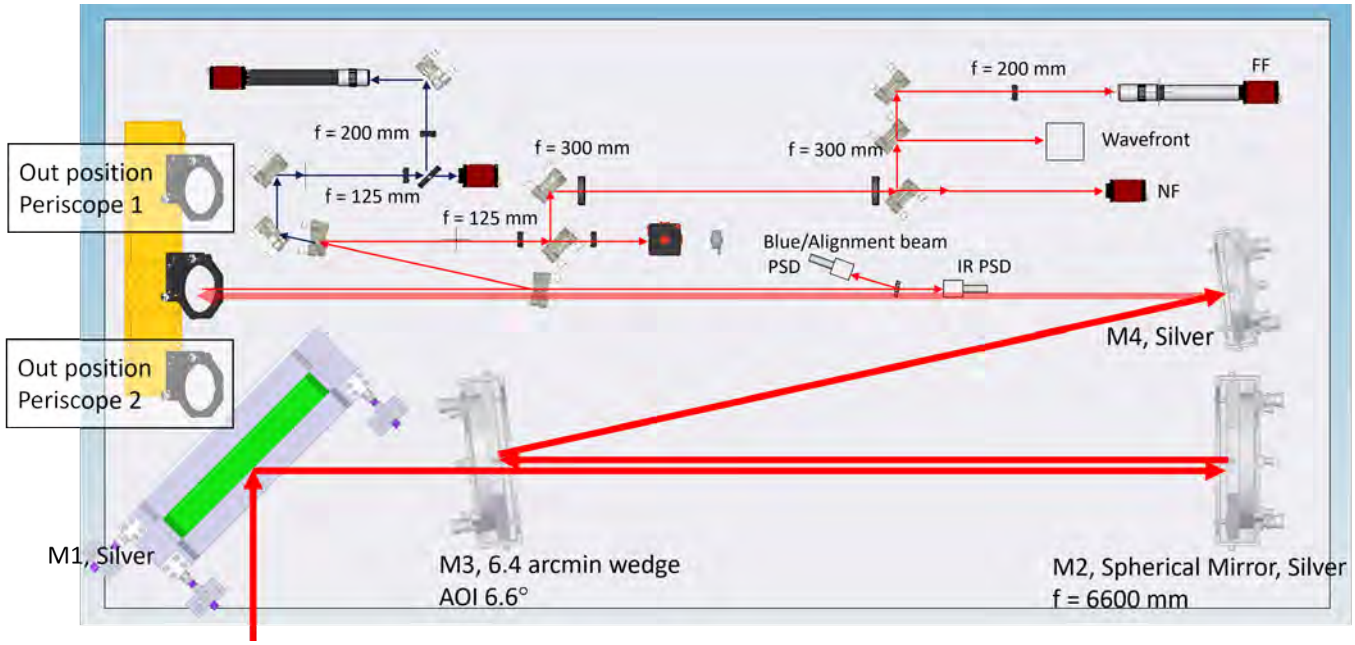

Figure 1: Proposed design for the diagnostic layout used for monitoring the beam entering the EA1 beamline

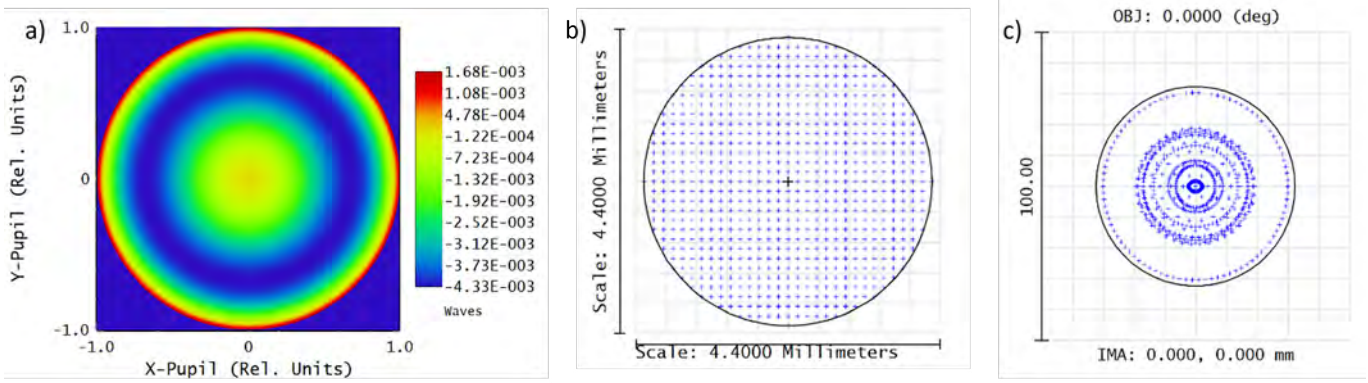

15 mm Aperture
RMS radius = 17 µm

Figure 2: (a) Wavefront map, (b) beam footprint, and (c) raytrace at the image plane of the main beam monitoring diagnostic

Bayesian Optimisation Guided PIC Simulations for EPAC

Experimental Area 1 at the Extreme Photonics Applications Centre (EPAC) will predominantly be used for electron acceleration in underdense plasmas. A mixture of permanent magnet and electromagnetic quadrupoles will be used to collect and transport electrons from the source to the application area or to diagnostics. To aid the design of the magnetic beamline, Particle-In-Cell (PIC) simulations have been performed to generate realistic electron beam outputs from the EPAC laser wakefield accelerator.

A high quality 1 GeV electron beam has been simulated and will be used as the input to magnetic tracking simulations.

Authors: O.J. Finlay, N. Bourgeois, D.R. Symes

Contact author: O. Finlay (oliver.finlay@stfc.ac.uk)

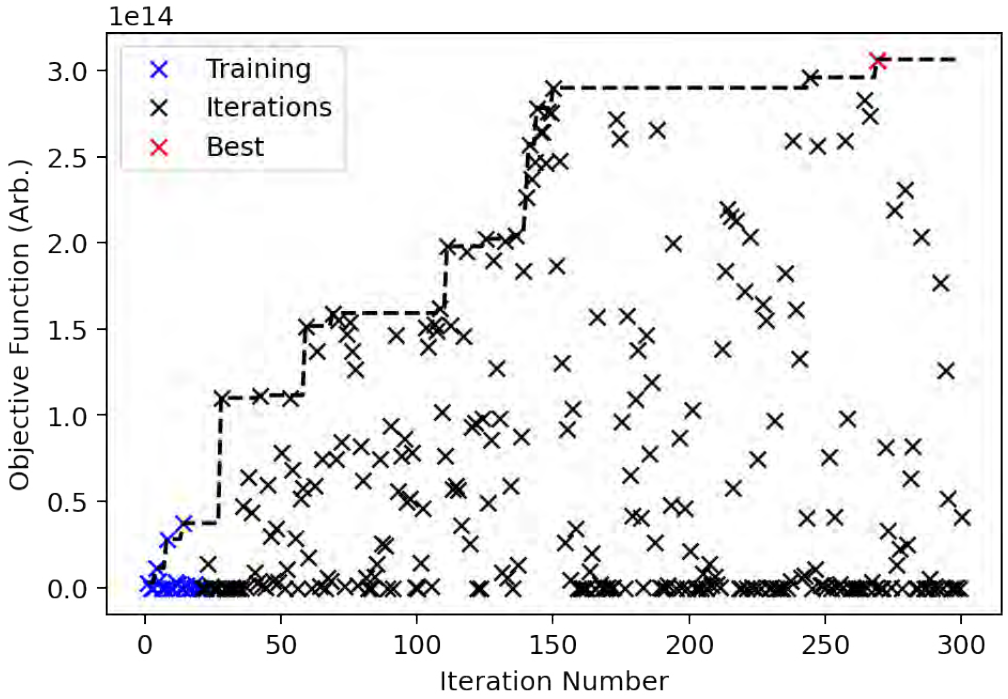

Figure 1: Objective function plotted against iteration number for a PIC simulation optimisation run

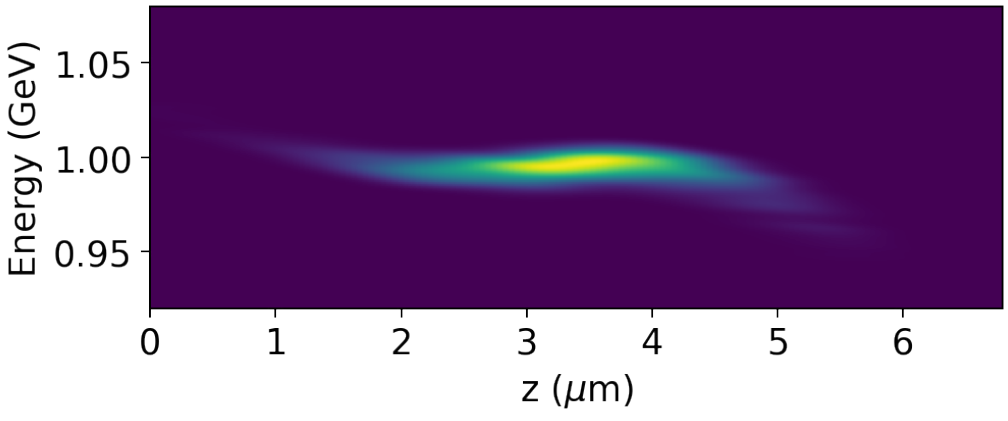

Figure 2: The longitudinal phase space of the optimised electron bunch

Vibration Survey and Analysis on EPAC Support Structures for Stability

This report presents the vibration survey for the new EPAC building, and the structure stability analysis for support structures and breadboards in the EPAC system.

The vibration survey was carried out after the construction of the EPAC building was finished, and before any laser equipment/ instruments were installed. This allowed the vibration of the building to be investigated and provided important data for future analysis in the EPAC system design. In addition, stability analysis was performed for critical structures including the high-level upper chamber and a breadboard for the target chamber. Vibration levels were investigated with the nearby ISIS laser facility both operating and not operating.

The results have enabled engineers to understand the dynamic behaviour of the key structures and evaluate the impact of vibration on the laser systems.

Authors: Z. Pan, S. Tomlinson, J. Bourne, N. Krumpa, A. Stallwood

Contact author: S. Tomlinson (steph.tomlinson@stfc.ac.uk)

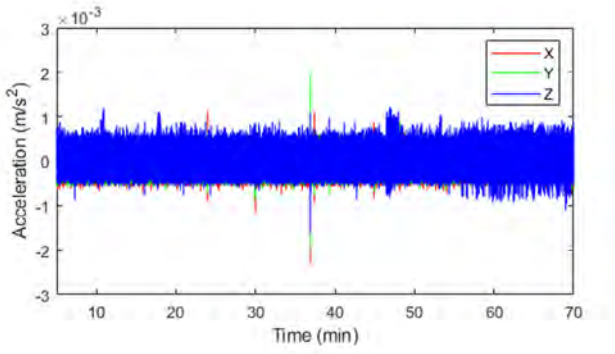

Figure 1: The acceleration of data captured on 26 July 2022 (nearby ISIS facility operating) shows that overall acceleration amplitudes across Experimental Area 1 are low, suggesting that the prevailing background vibration in the building is very low

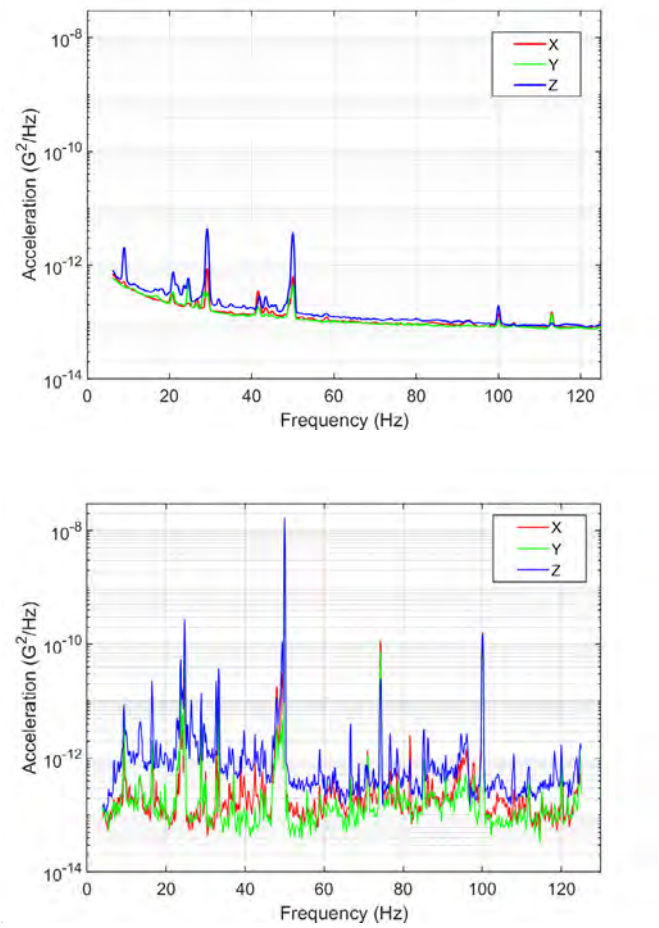

Figure 2: Measured power spectral density (PSD) for (top) Experimental Area 1 and (bottom) the Gemini area, captured with ISIS operational. The spectrum for EPAC is cleaner, with the peaks around 25, 50 and 100 Hz notably lower than those in the Gemini area.

High-repetition rate LWFA system in Gemini Target Area 2

During 2024/2025, in collaboration with our user community, we will use Gemini Target Area 2 (TA2) to carry out research and development necessary for prototyping and delivering EPAC. Construction of the LWFA beamline in TA2 will allow us to test components, and develop new techniques, in an iterative way that is not possible during short access slots on an operational user facility. We aim to continue studies of beam optimization through manipulation of a variety of factors, including plasma density, acceleration length, and laser pulse shape.

In this report, we describe elements of the experimental setup that have been developed for this purpose: the TA2 laser system and laser performance, the LWFA equipment, and available LWFA manipulation mechanisms.

Authors: K. Fedorov, D.R. Symes, C.D. Armstrong, S. Devadesan, O. Finlay, S.J.D. Dann, C. Selig, B. Spiers, N. Bourgeois, T. Dzelzainis. W. Robins, Z. Athawes-Phelps, R. Sarasola, D. Bloemers, I. Symonds, B. Morkot, A. Thomas, R. Lyon, T. Pocock, A. Gunn, T. Pacey, Y. Saveliev, S. Mathisen, A. Bhardwaj, R. Sugumar

Contact author: K. Fedorov (kirill.fedorov@stfc.ac.uk)

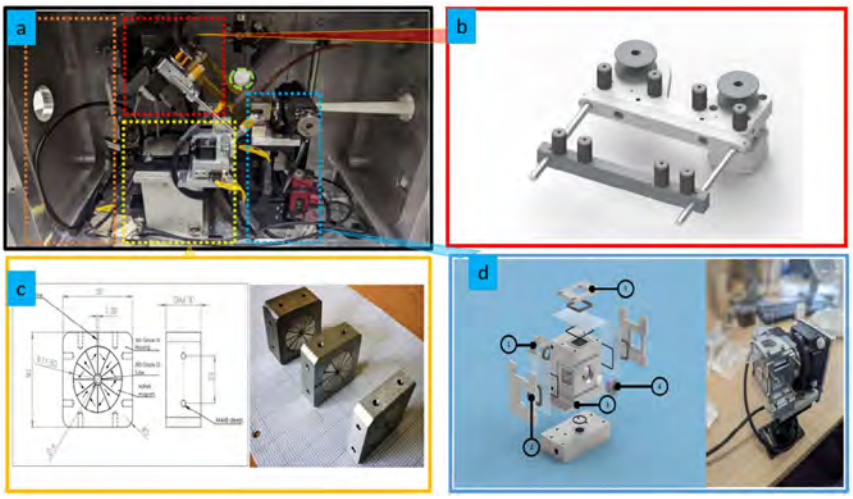

Figure 1: (a) The internal interaction chamber, colour-coded as follows: orange – space reserved for dielectric streaker; red – kapton tape drive/beam dump (shown in (b)); yellow – Halbach quadrupole magnet (shown in (c)) on XYZ translational stage; blue – gas-cell; (d) LEFT: Gas-cell assembly design: 1 – entrance aperture; 2 – probe beam diagnostics window; 3 – gas-cell volume; 4 – replaceable exit aperture MACOR plate; 5 – top view window; RIGHT: Assembly with a motorized stage to control gas-cell length

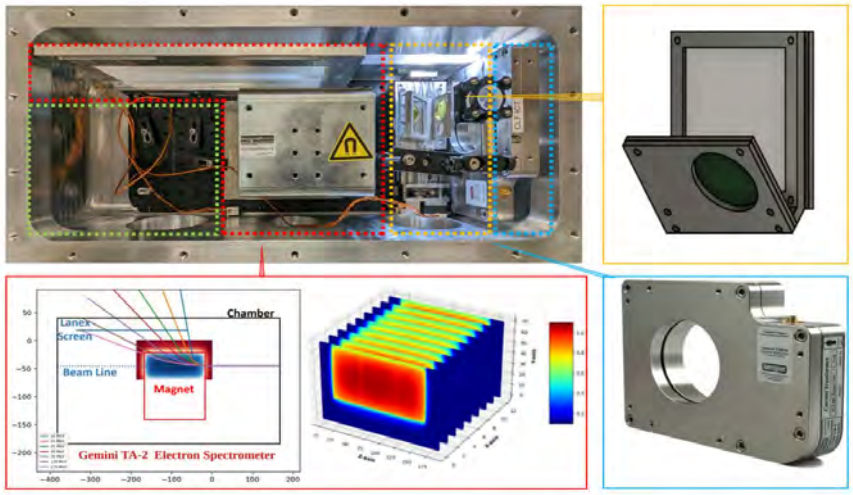

Figure 2: The diagnostics chamber developed to house specific diagnostics, colour-coded as follows: green – space reserved for tomography sample; red – electron spectrometer; orange – YAG:Ce scintillator screen; blue – integrated current transformer (Bergoz turbo-ICT)

Software developments in Gemini

The Gemini laser system's software undergoes upgrades to enhance control measures and facility monitoring. Leveraging EPICS enables the integration of diverter mirrors, pickoffs, and attenuators into the control system, streamlining experiment processes and enhancing safety. Expanded EPICS process variables (PVs) facilitate comprehensive facility-wide parameter monitoring, aiding in system health assessment. The redesigned facility monitoring application, penguin, provides real-time insights into system performance and experiment progress. These advancements optimize control and monitoring, ensuring safer and more efficient experimental operations.

Author: V.A. Marshall

Contact author: V.A. Marshall (victoria.marshall@stfc.ac.uk)

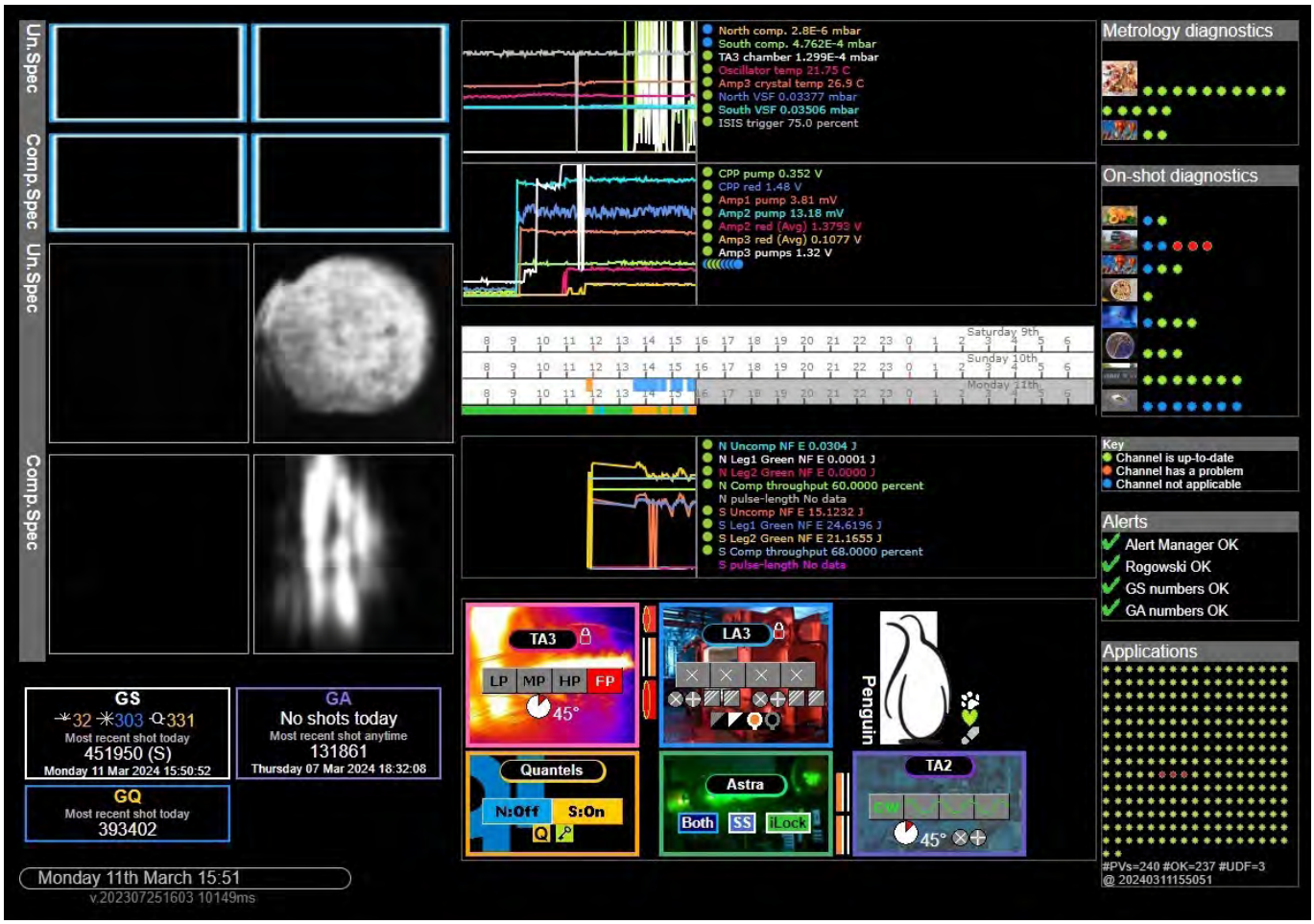

Screenshot of the main facility monitoring application – *penguin* – web page, which has been restructured and rewritten to take advantage of new features

Gemini timing drift stabilisation

A new method of analysis was implemented to improve timing drift stabilisation on Gemini, measuring delay on individual measurements of drift with an uncertainty of 9 fs. Code was written to move the split and delay stage in order to compensate for drift; in typical operating conditions, delay due to drift was kept smaller than delay due to shot-to-shot jitter.

Authors: P. Parsons, N. Bourgeois

Contact author: P. Parsons (pparsons03@qub.ac.uk)

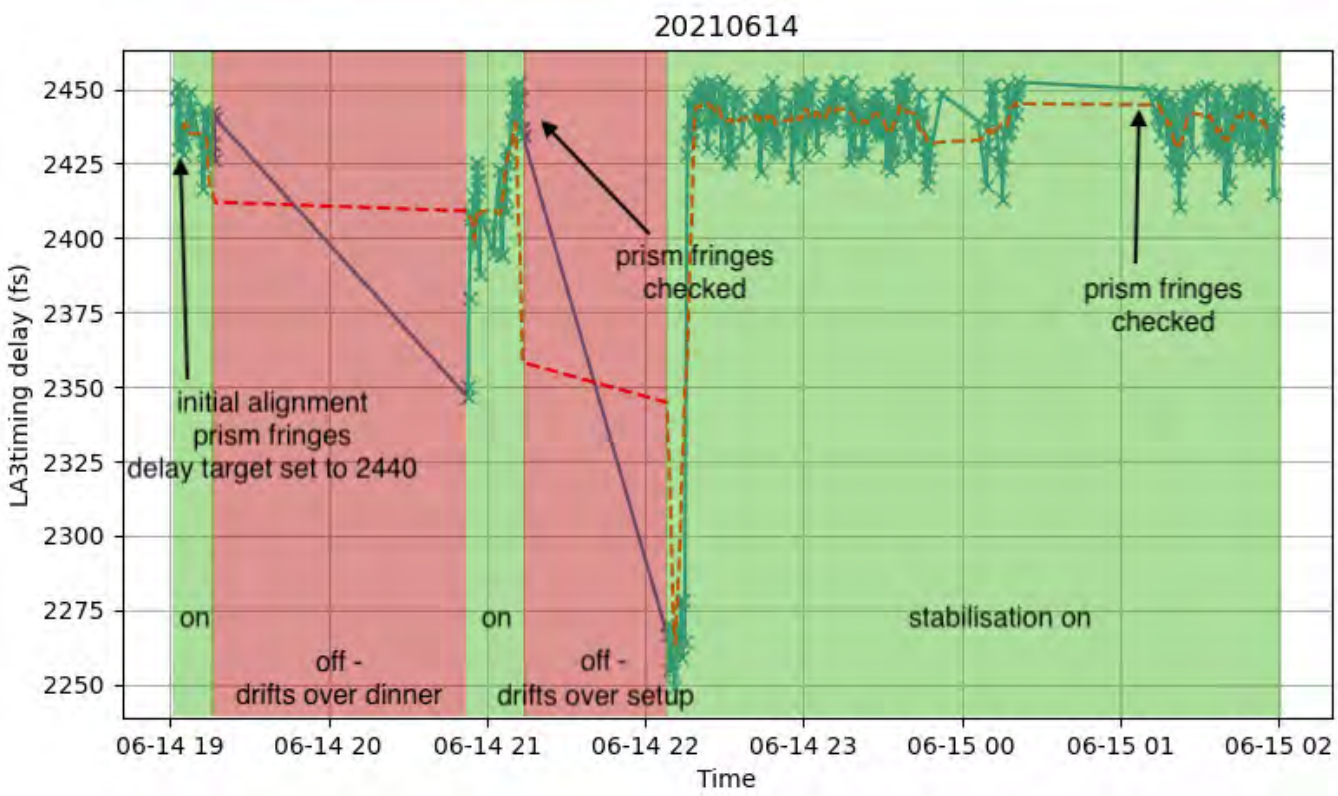

The delay between the two beams as measured in the laser area, LA3, against time. The green crosses are full power shots, and the red line is the 15 shot average. The timing stabilisation code was set to keep the drift at 2440 fs and was running except for the two red sections at about 7:15pm and 9:15pm. 'Prism fringes checked' refers to confirming the delay by measuring it in the target area with using a prism and spatial interference – these gave a similar values to the timing diagnostic in LA3.

Graph courtesy of C. Colgan, Imperial College London

Commissioning Progress of the New Petawatt Beamline in Vulcan

A new, short pulse petawatt beamline was successfully installed into R1 to accompany the Vulcan laser. The layout and progress are discussed, with the various commissioning challenges and accomplishments.

Authors: S. Buck, V. Aleksandrov, P. Oliveira, M. Tobiasiewicz, T. Winstone, M. Woodward, M. Galimberti

Contact author: S. Buck (samuel.buck@stfc.ac.uk)

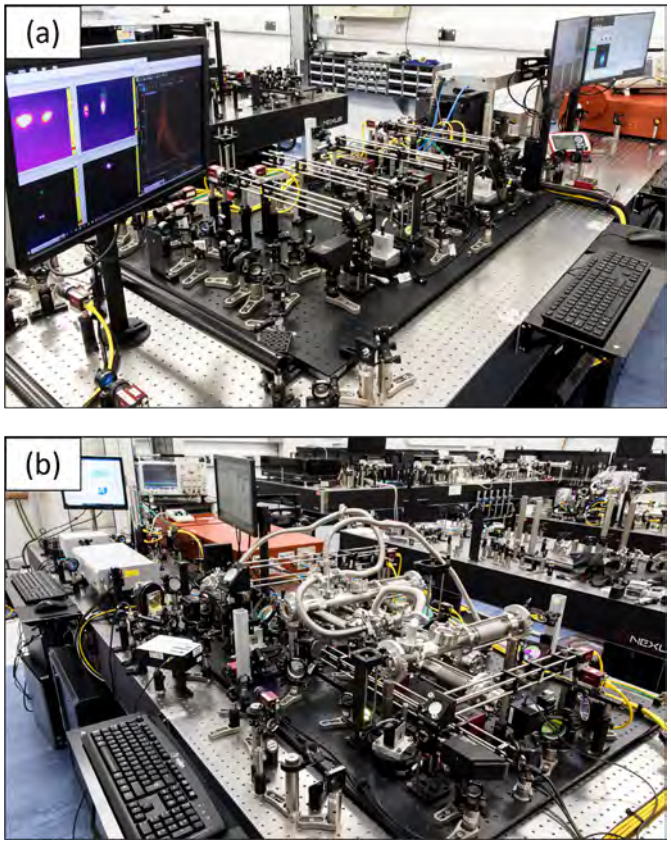

Figure 1: Picosecond front end of the VOPPEL beamline: (a) Stages 1 and 2, (b) Stages 3 and 4

Figure 2: Three-tier table installed in LA4. A large-aperture (90 mm) LBO OPA stage on the bottom level will be pumped by a frequency-converted Vulcan long pulse beam, delivered from the top level.

Single shot autocorrelator for the emPULS laser system

In the Laboratory for Advanced Analytical Technologies of the Swiss Federal Laboratories for Materials Science (Empa), a new terawatt laser facility (emPULS) is under development. The system is a CPA architecture based on Nd:phosphate flash pumped amplifier, similar to the rod chain of the Vulcan laser system. Within the scientific collaboration, a single shot autocorrelator was setup, following the successful design of the pulse front tilt single shot autocorrelator developed at CLF.[1]

[1]*Gonçalo Figueira et al. "Simultaneous measurement of pulse front tilt and pulse duration with a double trace autocorrelator," J. Opt. Soc. Am. B 36, 366-373 (2019). doi: 10.1364/JOSAB.36.000366*

Authors: Y. Hemani, D. Bleiner, M. Galimberti

Contact author: M. Galimberti (marco.galimberti@stfc.ac.uk)

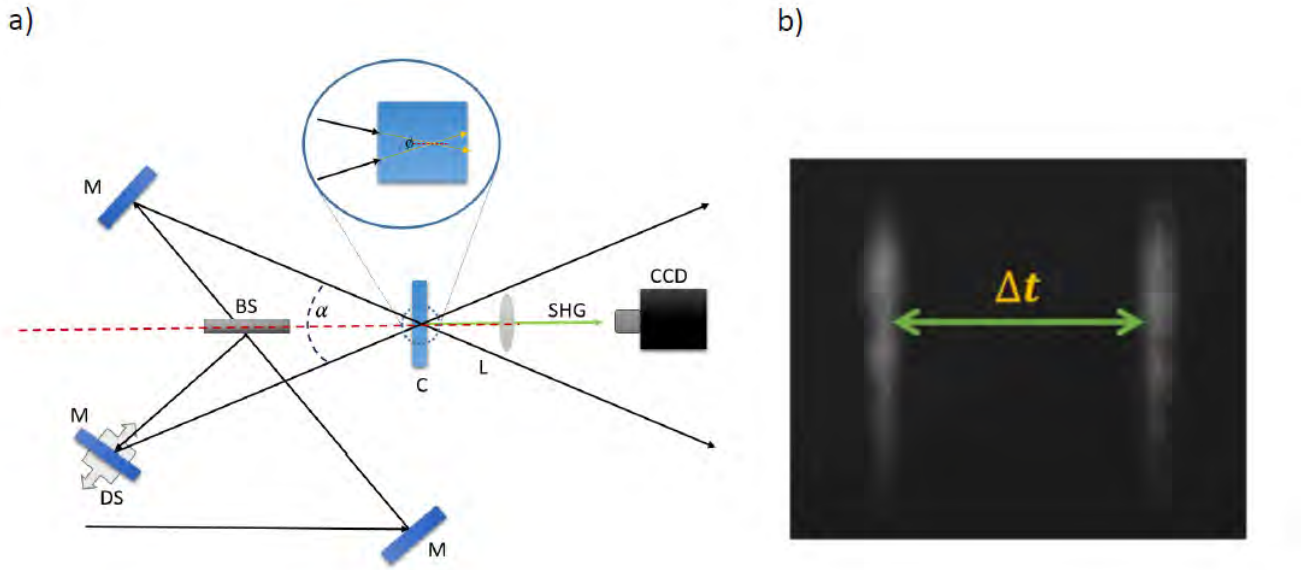

Figure 1: a) Optical design of a single shot auto correlator. It consists of: three mirrors (M), of which one is on a delay stage (DS); a beam splitter (BS); a non-linear crystal (C); a focusing lens (L); and camera (CCD). b) An example of an auto-correlator measurement is shown. The separation between two reflected pulses is indicated.

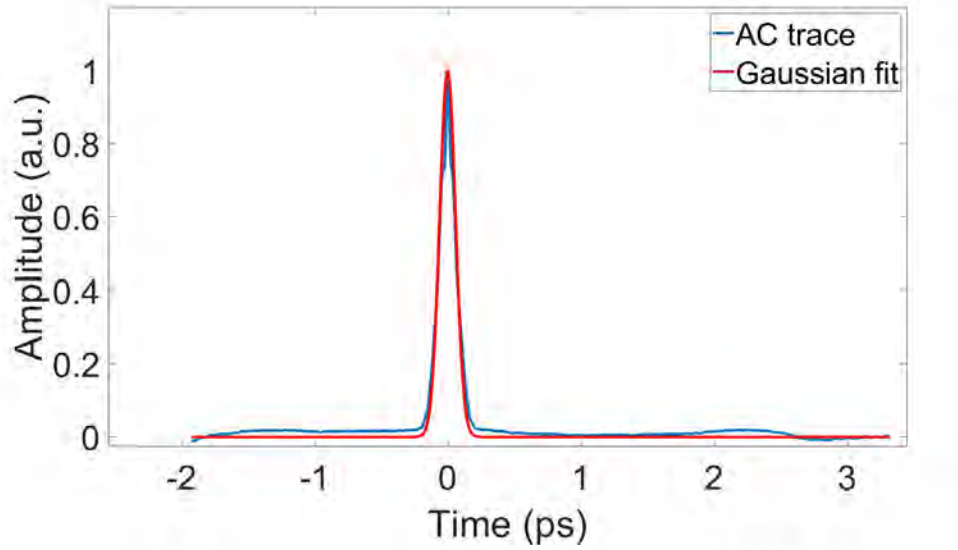

Figure 2: The calibrated autocorrelation trace collected from the camera is shown (in blue), with its Gaussian fit (in red)

Reduction of electrical noise on diode trace measurements via a pulse replicator

A low cost and easy to implement solution to increase the signal to noise ratio in single shot measurements is presented. Pulse replicas are created and redistributed to the same photodiode/oscilloscope combination. Averaging those replicas reduces the electrical noise in the pulse shape. We present simulation and experimental results including a calibration of the instrument.

Authors: A. Mayouf, P. Oliveira

Contact author: P. Oliveira (pedro.oliveira@stfc.ac.uk)

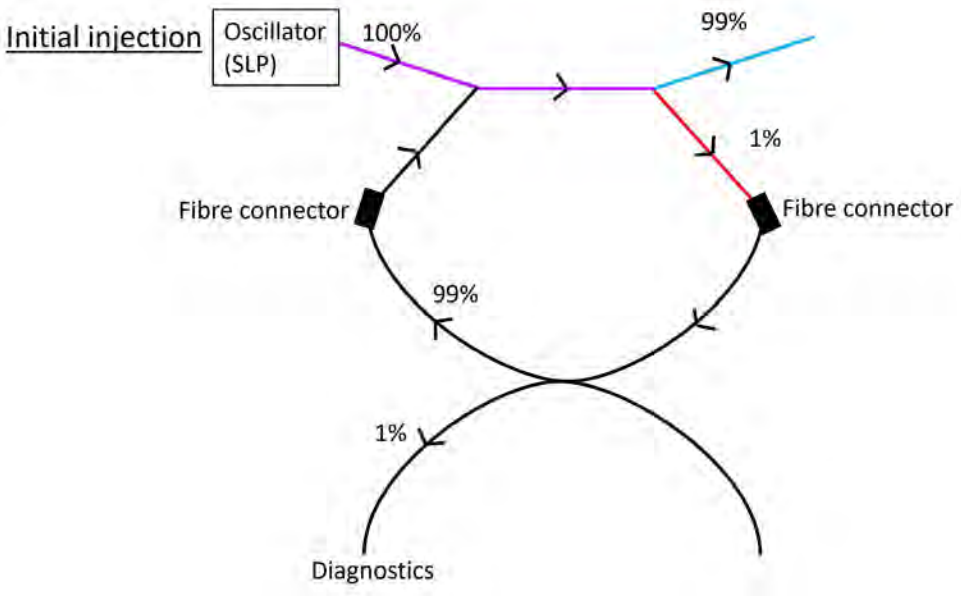

Figure 1: Fibre system setup showing initial injection from the oscillator into the two fibre splitters, which had been connected together then into the diagnostics. The percentages of the intensity of light going through each section of the fibre system are shown.

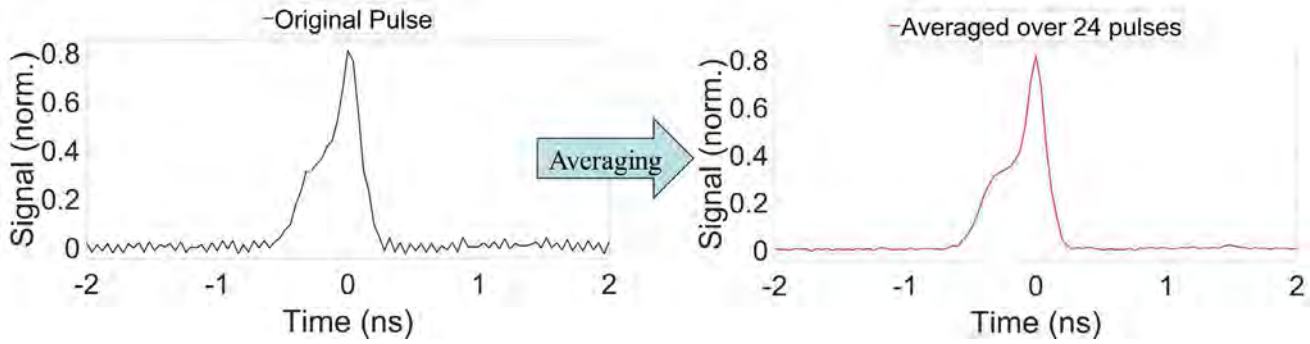

Figure 2: Pulse shape before averaging (left) compared with the pulse shape after optimal averaging (right).

Characterisation of Nested Anti-Resonant Hollow Core Fibre for Ultrafast Synchronisation Applications

In this report, a new nested anti-resonant nodeless (NANF)-type hollow core fibre (HCF) cable has been made and characterised for use in the Vulcan Petawatt Laser Facility. First measurements of the autocorrelation, spectrum and spectral interferogram of light directed through 50 m of the fibre demonstrate its ability to distribute laser pulses with little change over distances relevant to the scale of the Vulcan 20-20 facility. The results support its use as a distributor of optical reference pulses for the Vulcan 20-20 timing system.

Authors: A.C. Aiken, J.R. Henderson, P. Oliveira, J. Morse, M. Galimberti, B. Shi, F. Poletti, R. Slavik

Contact author: P. Oliveira (pedro.oliveira@stfc.ac.uk)

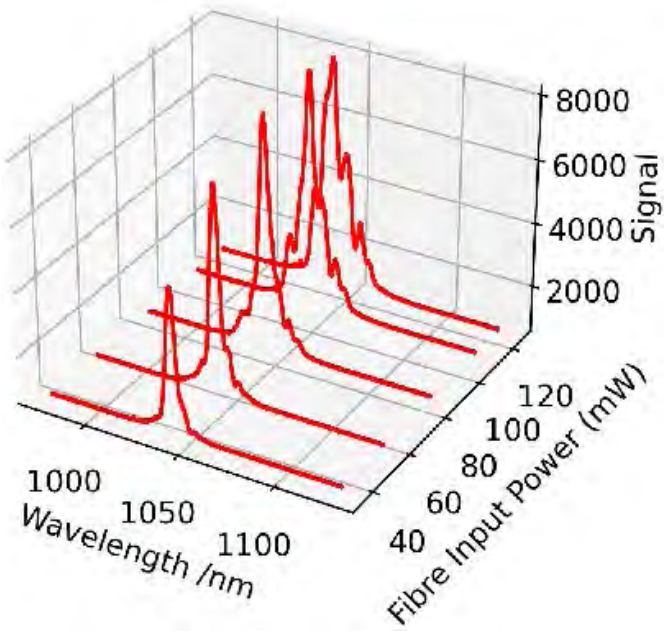

Figure 1: Evolution of the spectral envelope of the light with increasing power coupling into the fibre

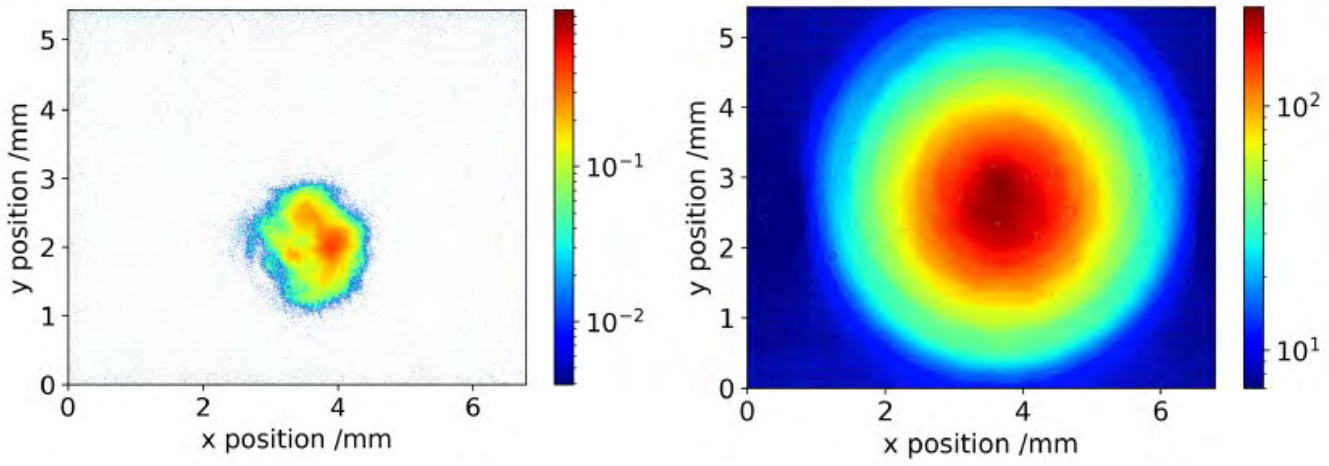

Figure 2: (Left) Spatial profile of the InSight DeepSee ultrafast laser prior to the fibre input. (Right) Spatial profile at the output of the fibre. Image colour scales are arbitrary.

A versatile high-average-power ultrafast infrared driver tailored for high-harmonic generation and vibrational spectroscopy

Ytterbium-based high-average-power lasers are becoming increasingly popular amidst the ultrafast science community. They afford robust and reliable turn-key operation at high repetition rates with sufficient laser pulse energies to drive non-linear phenomena in atoms, molecules and condensed matter. We recently commissioned a tunable infrared femtosecond optical parametric chirped-pulse amplifier, driven by a 200 W (2 mJ at 100 kHz) thin-disk regenerative amplifier at a wavelength of 1 micron. The laser is tailored to suit a wide variety of experimental requirements for Ultra and Artemis, ranging from ultrafast infrared and Raman spectroscopy to transient angle-resolved photoelectron spectroscopy (tr-ARPES) and x-ray absorption spectroscopy (tr-XAS) using high-harmonic generation (HHG). The versatility of the laser design provides a feasible means of investing into a single high-average-power front-end and yet be able to cater to diverse experimental platforms in ultrafast condensed-matter physics, material science, chemistry and biology.

Authors: N. Thiré, Y. Pertot, O. Albert, N. Forget, G. Chatterjee, G. Karras, Y. Zhang, A.S. Wyatt, M. Towrie, E. Springate, G.M. Greetham

Contact author: G. Chatterjee (gourab@slac.stanford.edu)

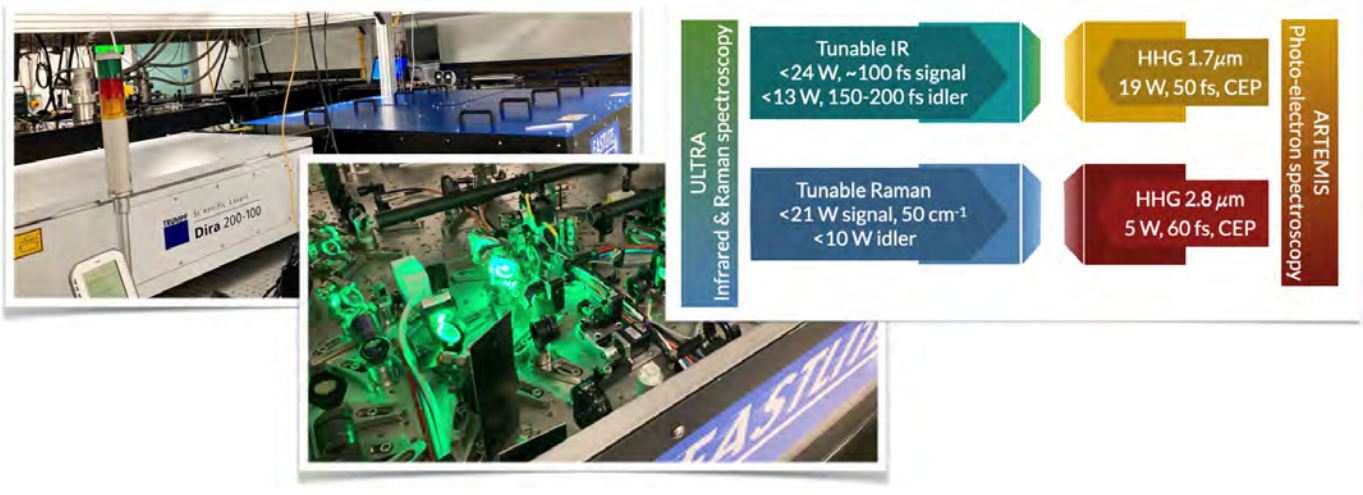

Generation and characterisation of <10 fs pulses for ultrafast spectroscopy in Ultra

Sub-10 fs pulses for driving two-dimensional electronic spectroscopy (2DES) experiments at the Ultra facility have been produced and characterised, using a combination of hollow core fibre pulse broadening and a commercial dispersion scan system. This source will initially be for use in 2DES, but it opens the door to a range of other broadband time-resolved spectroscopies.

Authors: T.B. Avni, G. M. Greetham, I.A. Heisler, S.R. Meech

Contact author: T.B. Avni (timur.avni@stfc.ac.uk)

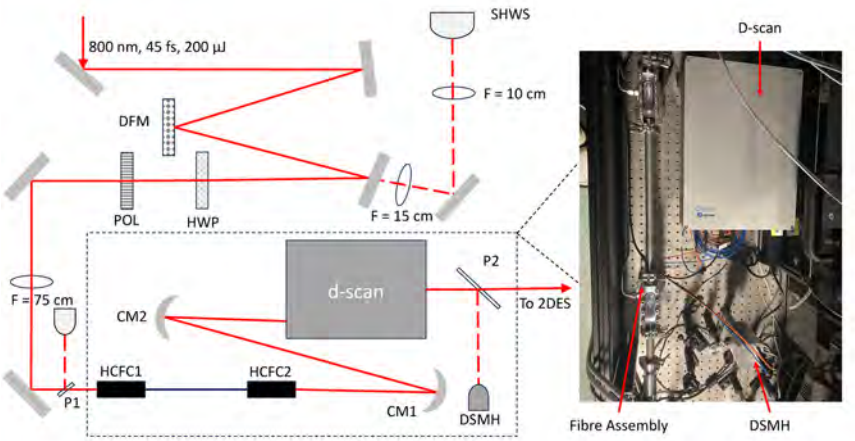

Figure 1: (Left) Schematic of the beam path to the hollow core fibre and the diagnostics before and after it to prepare the beam for use in 2DES experiments. The solid lines represent the primary beam path, and the dashed lines are leak-through and pickoff beams for diagnostics. (Right) The fibre and d-scan as installed in Ultra-B.

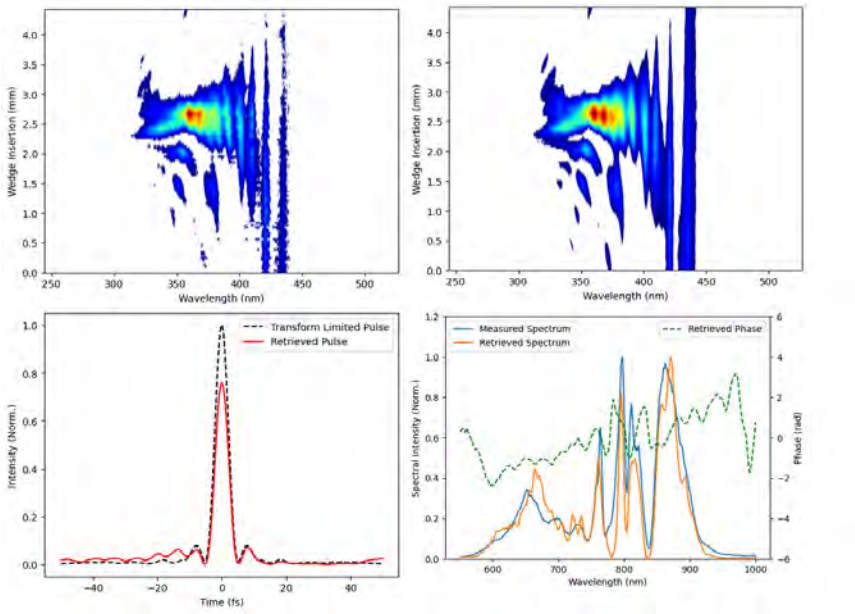

Figure 2: Diagnostic data from measurements taken with the d-scan. Top-left: The measured d-scan trace, showing spectrum vs thickness of glass insertion, with optimal compression seen at 2.8 mm wedge insertion. Top-right: The reconstruction of the measured trace using proprietary reconstruction algorithms. Bottom-left: The reconstructed (orange) vs measured (blue) spectrum at the point of optimal pulse compression, overlayed with the retrieved spectral phase (green, dashed). Bottom-right: The retrieved temporal intensity of the pulse (red) and the ideal transform limited pulse (black, dashed). The reconstruction gives a pulse duration of 4.75 fs, with a transform limit of 4.68 fs and a reconstruction error of 1.9%.

Half-broadband two-dimensional electronic spectroscopy with active noise reduction

Two-dimensional electronic spectroscopy (2DES) provides detailed insight into coherent ultrafast molecular dynamics in the condensed phase. Here we report a referenced broadband pump-compressed continuum probe half-broadband 2DES spectrometer in a partially collinear geometry. To optimise signal-to-noise ratio (SNR) we implement active noise reduction referencing. The method is calibrated against the well characterised 2DES response of the oxazine dye cresyl violet and demonstrated at visible wavelengths on the photochromic photoswitch 1,2-Bis(2- methyl-5-phenyl-3-thienyl)perfluorocyclopentene (DAE). The SNR is improved by a factor of ~2 through active referencing. We further show that active noise reduction referencing, coupled with the rapid data collection, allows the extraction of weak vibronic features, most notably a low frequency mode in the excited electronic state of DAE.

Authors: G. Bressan, S.R. Meech, I.A. Heisler, G.M. Greetham, A.E.D. Meades

Contact author: S.R. Meech (s.meech@uea.ac.uk)

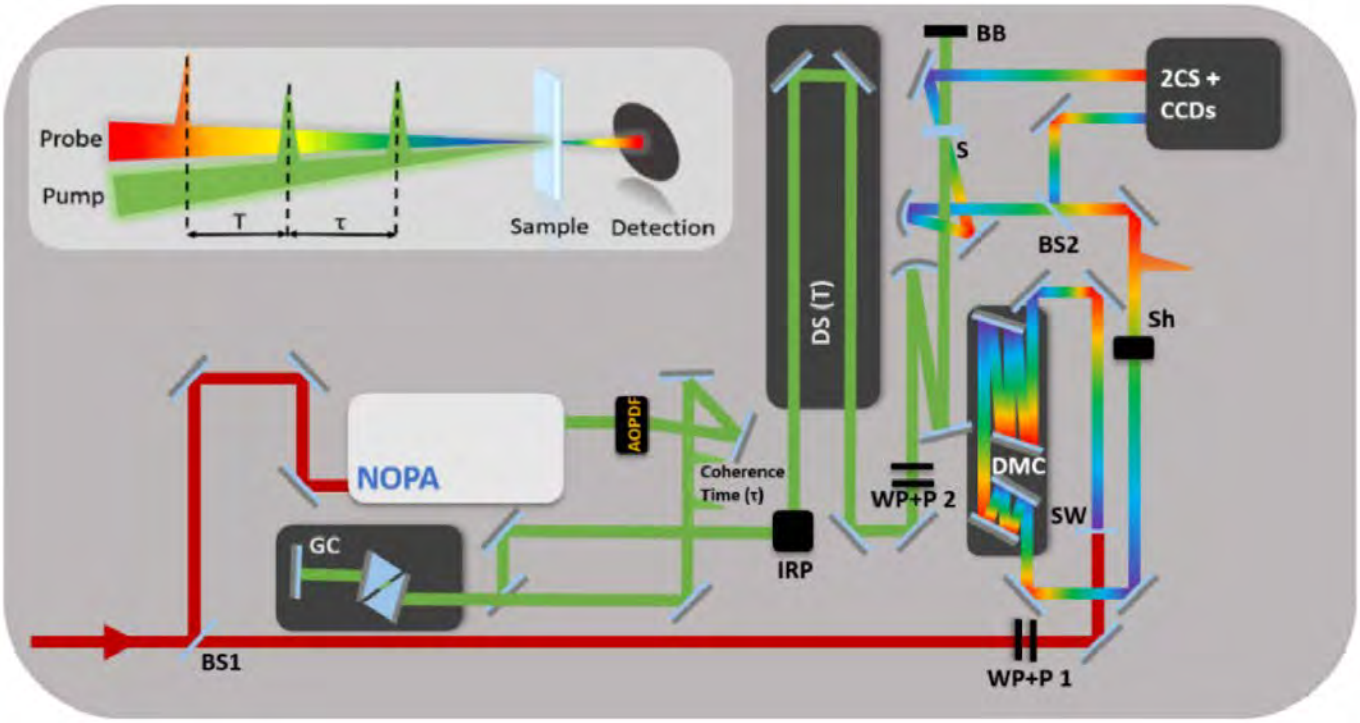

Complex Micro-Target Fabrication to Study Shock Compression

Recent years have seen target complexity increase due to the availability of a greater range of diagnostic techniques, and also because of the general growth in sophistication of experiments that are conducted. Target fabrication for such experiments typically requires integration of a range of techniques to make one target cluster. To meet demand, there has been a rapid development in advanced target fabrication techniques such as robotic assembly, micro 3D printing, single-point diamond turning, laser micromachining and (MEMS-based) lithography.

This annual report details one complex target fabrication programme that was carried out for an experiment in Target Area West on the Vulcan facility.

Authors: P. Ariyathilaka, D. Wyatt, C. Spindloe, M. Tolley, M. Oliver, L. Sparkes, B.C. Bateman

Contact author: P. Ariyathilaka (pawala.ariyathilaka@stfc.ac.uk)

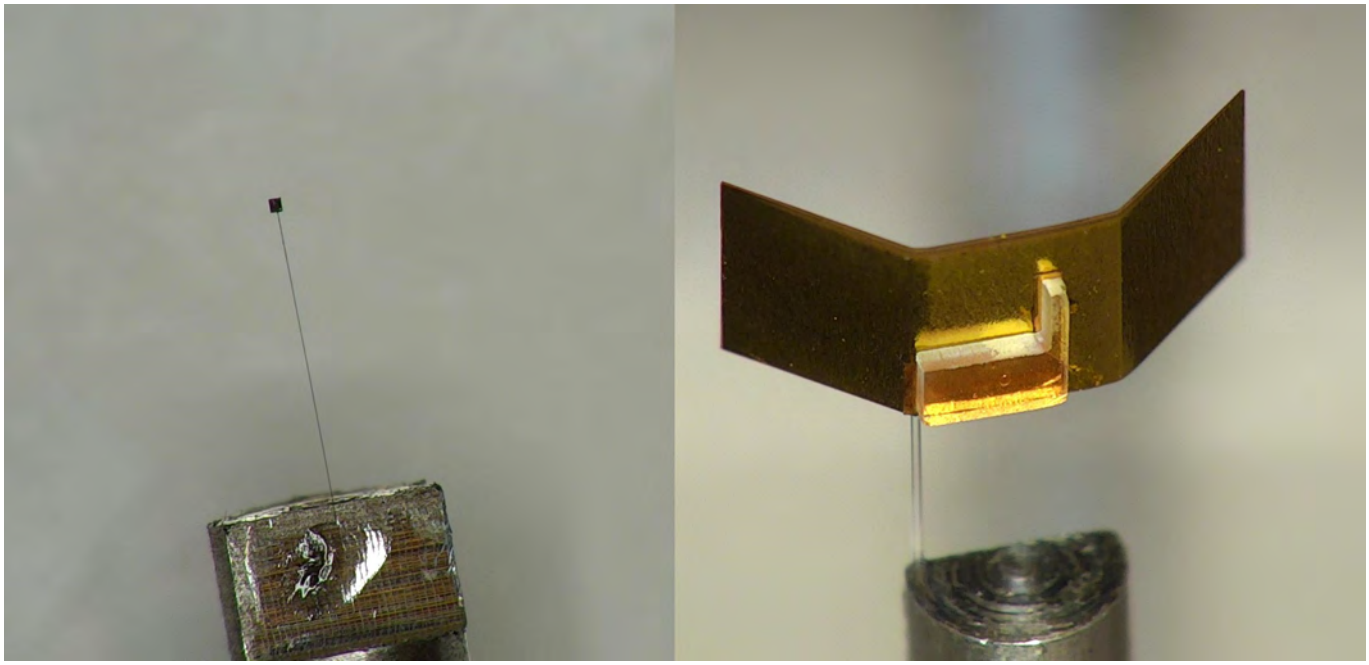

Two of the three targets used in the final target cluster: (left) Zinc backlighter foil 100 µm x 100 µm, and (right) lithium fluoride sample assembled to gold shield

Liquid Targetry Development for High Repetition Rate Experiments

The demands of modern high repetition rate, high power lasers have ushered in new challenges for laser targetry. For applications in X-ray free electron lasers and for plasma mirror experiments, thin liquid sheet targets have proven themselves to be perfect candidates due to their low debris and ability to rapidly self-replenish. The Extreme Photonics Applications Centre (EPAC) will come online within the next couple of years, and we face the need to develop larger and thinner sheets than previous studies have achieved. However, fine tuning nozzles via a system of trial and error is a long and costly process.

Here, we propose an efficient pipeline from conception of a design through simulation and optimisation, prototyping and testing, and finally production of a functioning part ready for application in high power laser experiments. We outline the progress made so far and the next steps required to make this a functioning process ready for implementation.

Authors: D.E. Crestani, S. Astbury, H. Edwards, W. Robins, C. Spindloe, M. Beardsley, L. Bushnell, C. Palmer, P. Parsons

Contact author: D. Crestani (dominic.crestani@stfc.ac.uk)

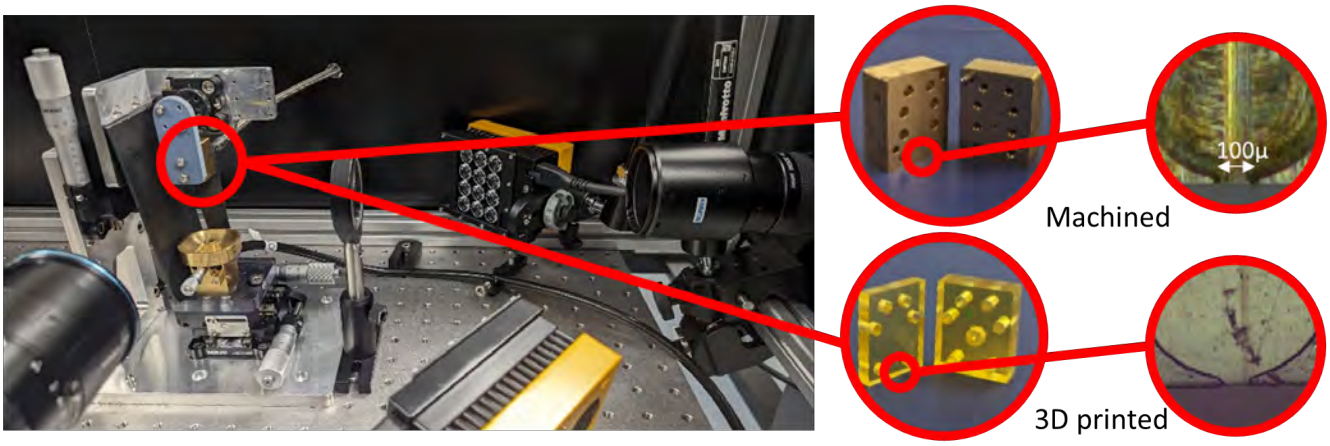

Figure 1: Experimental setup of the liquid target system, with magnified images of a high precision machined brass nozzle and a resin 3D printed nozzle

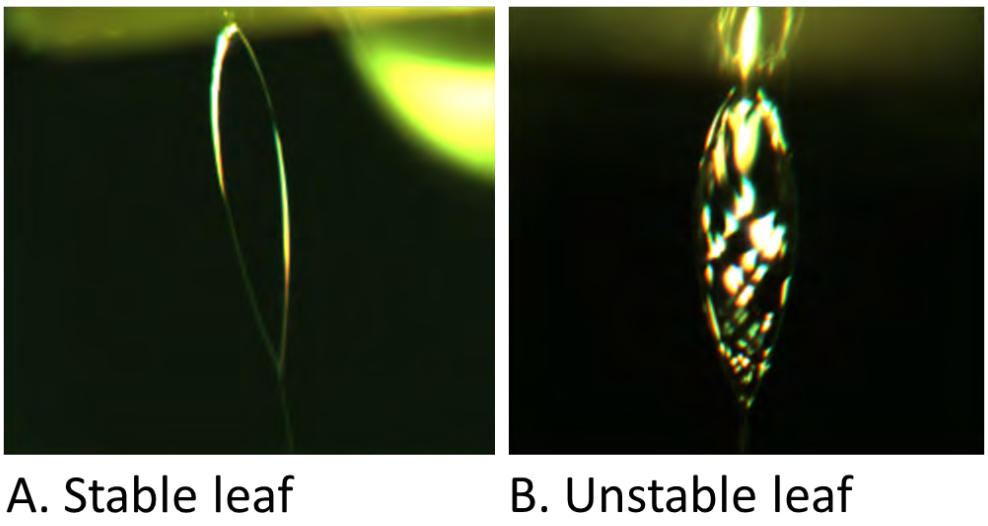

Figure 2: White light reflectance interferometry of a stable and an unstable liquid leaf

Using Additive Manufacturing to Aid the Manufacture of Complex 3D Microtargets

This article discusses the recent upgrades to the Target Fabrication group's suite of 3D printers, with the purchase and commissioning of a new micro additive manufacturing system and will give examples of where it has been used for target production.

The capability to print components with high resolution has opened many opportunities in target design. It has enabled more complex and, simultaneously, more flexible geometries to be made.

Moreover, it has often reduced or eliminated the need for assembly fixtures by producing multi-component assemblies in one print. Sets of components and complete laser microtarget assemblies have been printed.

Authors: C. Dobson, P. Ariyathilaka, D. Crestani, C. Spindloe, J. Robinson

Contact author: C. Dobson (claire.dobson@stfc.ac.uk)

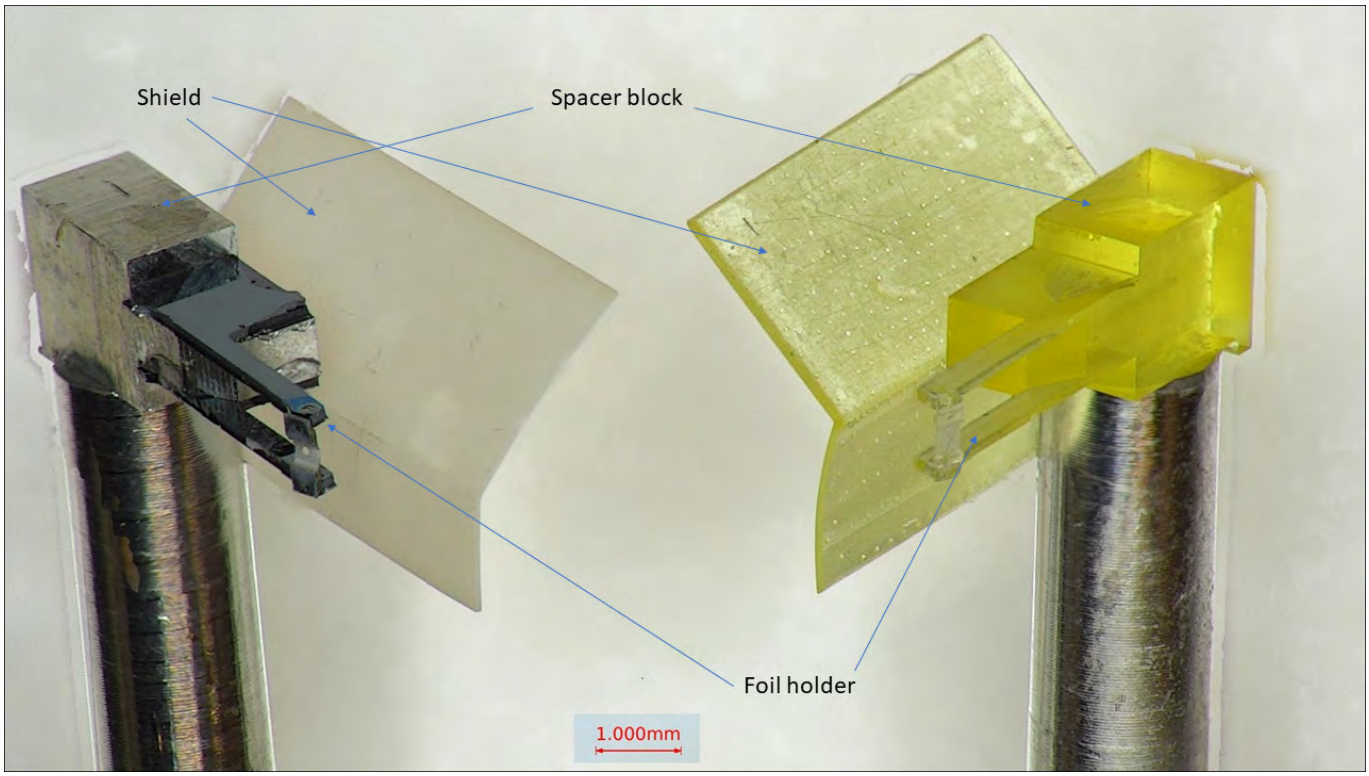

Traditionally made (multi-component) experimental target (left) and proof of concept 3D printed target (right). In this example, it was possible to print up to 90% of the target using the printer – including the spacer block, the foil mounts, and the shield on the rear of the target.
Photo: P. Ariyathilaka

Current developments in the Target Array Assembly System

The Target Array Assembly System (TAAS) is a robotic system that is being developed by the Target Fabrication Group of the Central Laser Facility to autonomously assemble microtarget arrays. The project is being developed to support the future solid target demands of the Extreme Photonics Applications Centre (EPAC) facility, which will be operational in 2025 [1].

Currently, the TAAS can automatically assemble an array target containing 32 foils in 27 minutes. This milestone provided an opportunity to review the abilities and future development plans for the TAAS. In this article, the functional requirements for the system are set out, as well as the current layout of the system. The target assembly methodology and system design are described, before highlighting areas for future development work.

[1]P. Umesh et al, "A Systems Engineering Architecture for Robotic Microtarget Production", CLF Annual Report 2019-20

Authors: J. Fields, P. Ariyathilaka, S. Astbury, M. Tolley, C. Spindloe

Contact authors: J. Fields (jfields1@sheffield.ac.uk)

P. Ariyathilaka (pawala.ariyathilaka@stfc.ac.uk)

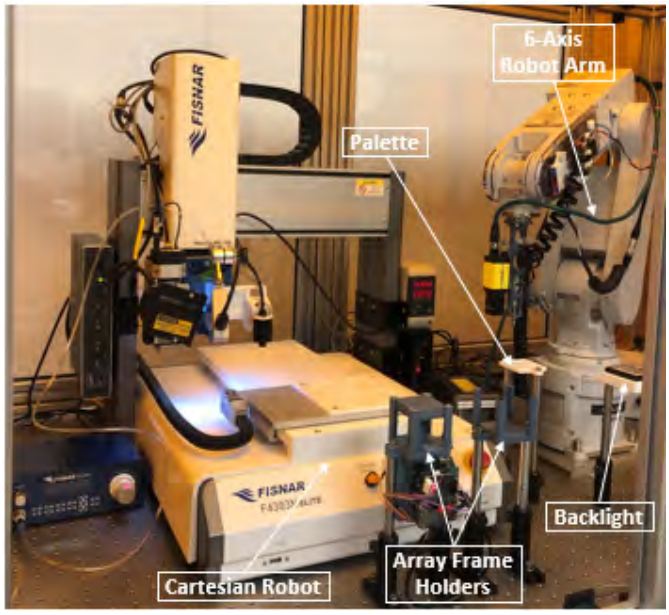

Figure 1: The Target Array Assembly System (TAAS), showing the robot arm, cartesian robot, array frame holders, backlight and palette

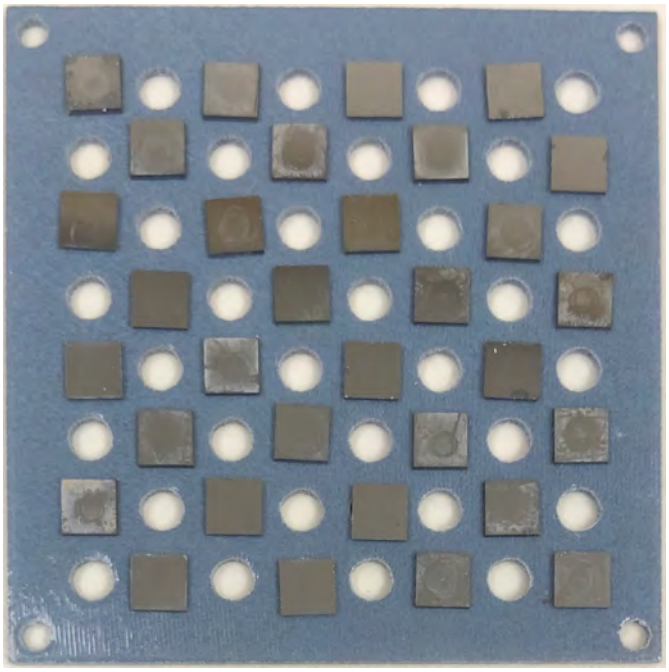

Figure 2: A '32-foil' array target

Investigating sources of inaccuracy within the Target Array Assembly System

The Target Array Assembly System (TAAS) is a robotic system that is being developed by the Central Laser Facility's Target Fabrication group to autonomously assemble microtarget arrays. A MELFA 'RV-2FRLB' industrial robot is used to manipulate target foils for the assembly of array targets. During system development, a coordinate drift was observed in this robot, causing unreliable and inaccurate foil placement. After initial experimentation, an investigation into the effect of thermal expansion on the robot arm was conducted.

The position change with respect to temperature was quantified using chromatic confocal distance sensors. By measuring the relative distance between set positions on the robot and fixed reference positions, any position changes could be observed.

The investigation showed that thermal expansion caused a significant, yet repeatable, position change. This led to the development of a 'warm-up' routine for the arm, to ensure it was at an operation temperature before use. This experiment also provided a greater understanding of inaccuracies within the TAAS.

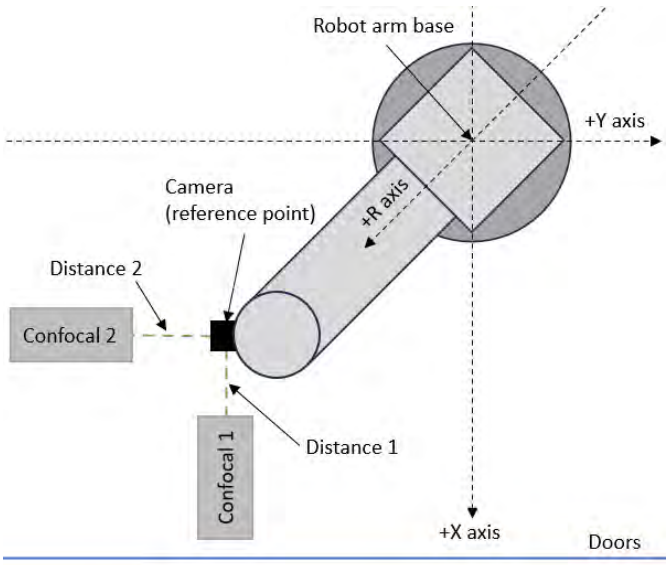

Figure 1: A simplified representation of the experimental setup

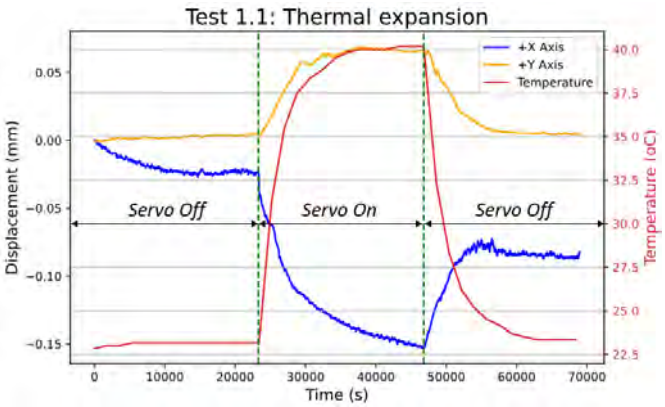

Figure 2: Change in position and temperature over time during one of the tests

Authors: J. Fields, P. Ariyathilaka, S. Astbury, M. Tolley, C. Spindloe

Contact authors: J. Fields (jfields1@sheffield.ac.uk)

P. Ariyathilaka (pawala.ariyathilaka@stfc.ac.uk)

Embedding of Ruby Microspheres in Low Density Foam Targets

Trimethylolpropane triacrylate monomer was used to create low density, polymeric structures by a supercritical fluid drying process to hold ruby microspheres for shock experiments. The design and manufacture of the target, and the initial results of the laser shock experiment, are covered by this article.

Ruby was chosen due to its density and average Z; challenges to ensure placement and fixing are covered. Full characterisation of the external and internal morphology of the target was conducted, with a combination of optical microscopy and x-ray radiographic measurements. The targets were successfully shot on the PHELIX laser in GSI.

Authors: S. Irving, P. Ariyathilaka, C. Spindloe, J. Robinson, P. Neumayer, L. Wegert

Contact author: S. Irving (samuel.irving@stfc.ac.uk)

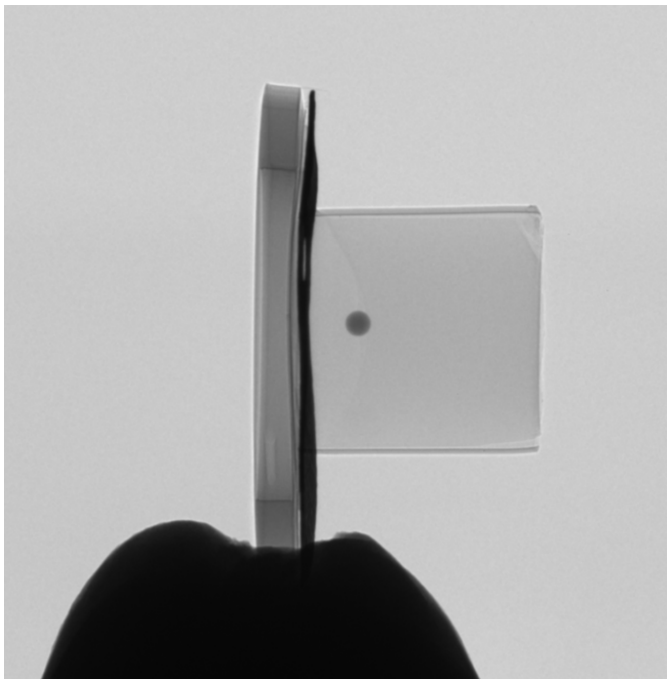

Figure 1: Side on radiograph with a much-reduced interfacial membrane

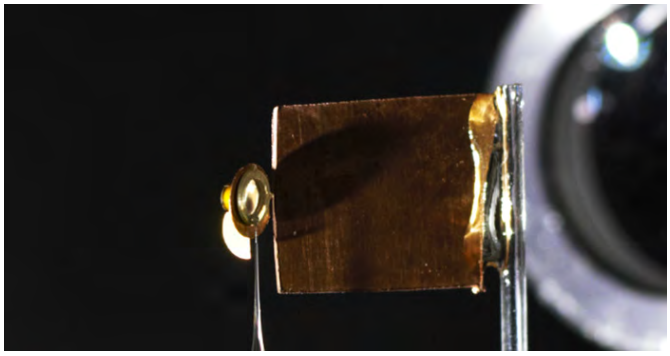

Figure 2: The target in the chamber (left) with additional shielding (right)